The petrological control on the lithosphere-asthenosphere boundary (LAB) beneath ocean basins

Yaoling Niu[1,2,3,4*] David H. Green[5]

[1] China University of Geosciences, Beijing, China
[2] Department of Earth Sciences, Durham University, UK
[3] Institute of Oceanology, Chinese Academy of Sciences, China
[4] Qingdao National Laboratory for Marine Science and Technology, China
[5] School of Earth Sciences, University of Tasmania, Australia

Submitted November 3rd, 2017 to *Earth-Science Reviews*
Revised submission on June 12, 2018

Correspondence:
yaoling.niu@durham.ac.uk
Department of Earth Sciences, Durham University, UK

Keywords:
Lithosphere-asthenosphere boundary; LAB; Petrological control; Amphibole dehydration solidus; Petrologically facilitated sub-LAB convection; Plate model

Highlights:

- The lithosphere-asthenosphere boundary (LAB) beneath ocean basins is the dehydration solidus of pargasite (amphibole), whose stability defines the lithosphere with T ≤ ~ 1100°C, P ≤ ~ 3 GPa (~ 90 km) and H_2O < 0.02 wt%;

- The LAB is an isotherm with T ≈ 1100°C, whose depth L increases with age t, i.e., $L \alpha t^{0.5}$ for t < ~ 70 Ma because of conductive cooling to the seafloor;

- The LAB is an isobar at P ≈ 3 GPa (~ 90 km) for t > ~ 70 Ma, above which is the conductive lithosphere and below which is the convective asthenosphere, explaining why the lithosphere cannot grow any thicker when t > ~ 70 Ma and making sub-LAB convection possible.

ABSTRACT

The plate tectonics theory established ~ 50 years ago has formed a solid framework for understanding how the earth works on all scales. In this theory, movement of the tectonic plates relative to the subjacent asthenosphere is one of the fundamental tenets. However, the nature of the boundary between the lithosphere and asthenosphere (LAB) beneath ocean basins remains under debate. The current consensus is that the oceanic lithosphere thickens with age by accreting asthenosphere material from below, and reaches its full thickness (L) of ~ 90 km at the age (t) of ~ 70 Ma. This lithospheric thickening fits the relation $L \propto t^{1/2}$, consistent with conductive cooling to the seafloor. A puzzling observation is that although conductive cooling continues, the oceanic lithosphere ceases to grow any thicker than ~ 90 km when t > 70 Ma. Small scale convection close beneath the LAB has been generally invoked to explain this puzzle, but why such convection does not occur until L ~ 90 km at t > 70 Ma has been a matter of conjecture. In this paper, we summarize the results of many years of experimental petrology and petrological studies of oceanic basalts, which indicate consistently that the LAB is a petrological phase boundary marking the intersection of the geotherm with the solidus of amphibole (pargasite)-bearing lherzolite. That is, petrologically, the LAB is an isotherm of ~ 1100°C with $L \propto t^{1/2}$ for t < 70 Ma and an isobar of ~ 3 GPa (~ 90 km) for t > 70 Ma. This unifying concept explains why the LAB depth increases with age for t < 70 Ma and maintains constant (~ 90 km) for t > 70 Ma. The LAB, that is intrinsically determined by petrological phase equilibria, does not require small-scale convection. However, because the mantle above the LAB is the *conductive* lithosphere (pargasite-bearing lherzolite/harzburgite) and below the LAB is the viscosity-reduced *convective* asthenosphere (lherzolite/harzburgite + incipient melt), the small-scale convection in the asthenosphere close beneath the LAB under older seafloors becomes possible, whose *convective* heat supply balances the *conductive* heat loss, maintaining the constant heat flow, seafloor depth and lithosphere thickness.

1. Introduction

Plate tectonics is a unifying theory that unravels global geology and geological evolution as a consequence of Earth's cooling. The origin and evolution of the oceanic lithosphere best illustrate this cooling process (e.g., Sclater et al., 1980; Stein and Stein, 1992). Oceanic crust is formed at ocean ridges as the underlying asthenosphere ascends and undergoes decompression melting (e.g., McKenzie and Bickle, 1988). The basaltic melts so produced, when extracted, build the ocean crust with the peridotitic residues remaining in the mantle, accreting new growth to lithospheric plates (e.g., Niu, 1997). The movement of these plates, their subsidence and thickening with age by thermal contraction, and their eventual cycling back into the Earth's deep interior through subduction zones provide an efficient mechanism to cool the mantle, and is the primary driving force for mantle convection (e.g., Forsyth and Uyeda, 1975; Parsons and McKenzie, 1978; Davies and Richards, 1992; Stein and Stein, 1996). However, the nature of the boundary between the lithospheric plates and the subjacent asthenosphere (LAB) beneath ocean basins remains inconclusive despite many studies to this day (e.g., McKenzie, 1967; Sleep, 1969; Sclater and Francheteau, 1970; Lambert and Wyllie, 1968,1970; Green and Liebermann, 1976; Forsyth, 1977; Parsons and Sclater, 1977; Parson and McKenzie, 1978; Sclater et al., 1980; Wood and Yuen, 1983; Stein and Stein, 1992,1996; Phipps Morgan and Smith, 1992; McKenzie et al., 2005; Ballmer et al., 2007; Afonso et al., 2008a,b; Korenaga and Korenaga, 2008; Crosby and McKenzie, 2009; Fischer et al., 2010; Niu et al., 2011; Sleep, 2011; Grose and Afonso, 2013).

In this paper, we do not wish to go through many detailed arguments in these studies, but offer our understanding why the LAB is a petrological phase boundary built on many years of experimental petrology and oceanic petrogenesis largely done or led by the authors. To put the discussion in the context, we first concisely review the well-established observations and the prevailing view on the issue with caveats. We encourage both geophysical and modeling

disciplines to consider the petrological concept and the conclusion we offer here in their models towards a genuine understanding on the nature of the LAB.

2. Observations and physical foundation

Cooling of the Earth's mantle below the seafloor is well-understood because the correlated variations of heat flow observations, seafloor subsidence (D) and lithosphere thickness (L) with seafloor age (t) are effectively described by the half-space cooling model (HSM) $L \propto t^{1/2}$ (also $D \propto t^{1/2}$) with the base of the thickening lithosphere treated as an isotherm (e.g., Sclater and Francheteau, 1970; Lister, 1972; Parsons and Sclater, 1977; Parson and McKenzie, 1978; Sclater et al., 1980; Stein and Stein, 1992,1996; Phipps Morgan and Smith, 1992; Afonso et al., 2008a,b; Crosby and McKenzie, 2009; Sleep, 2011; Grose and Afonso, 2013) (Fig. 1). However, the seafloor depth reaches an asymptotic $D \approx 5.5$ km (the familiar "seafloor flattening") and the lithosphere reaches an asymptotic $L \approx 90$ km after $t \approx 70$ Ma (see Fig. 1; Scaler and Francheteau, 1970; Forsyth, 1977; Parson and McKenzie, 1978; Stein and Stein,1996; McKenzie et al., 2005; Afonso et al., 2008a,b; Korenaga and Korenaga, 2008; Crosby and McKenzie, 2009; Sleep, 2011; Grose and Afonso, 2013). Although conductive heat loss from the mantle continues with $t > 70$ Ma, there is apparently no further thickening of the lithosphere nor increasing depth to the seafloor. This apparent puzzle has led to many speculations, among which the plate model (PM vs. HSM) (e.g., Lister, 1972; Forsyth, 1977; Parson and McKenzie, 1978; Stein and Stein, 1996; McKenzie et al., 2005; Sleep, 2011) has gained general acceptance because it explains $L \propto t^{1/2}$ (and $D \propto t^{1/2}$) for seafloor with $t < 70$ Ma and approximately constant D and L for seafloor with $t > 70$ Ma. The PM is based on a proposition that the thickened lithosphere becomes unstable and small-scale convection triggered at the LAB raises the temperature, providing heat to prevent the lithosphere from thickening. A model invoking small-scale convection beneath older oceanic lithosphere has thus been widely applied at the

LAB and supported with numerical models of varying sophistication (e.g., Forsyth, 1977; Parson and McKenzie, 1978; Buck and Parmentier, 1986; Huang et al., 2003; Ballmer et al., 2007; Sleep, 2011). The simple question is why such convection does not occur until $L \approx 90$ km when $t \geq 70$ Ma. Before understanding the reason if any, we agree that such treatments are a constructive step forward, but they require two discrete functions with heat loss for $t < 70$ Ma ($L \propto t^{1/2}$) and excess heat supply to balance conductive heat loss for $t > 70$ Ma to prevent lithosphere from further thickening (ΔL (t) ≈ 0) with $L \approx 90$ km (e.g., Stein and Stein, 1996). Because thermodynamically, the material (e.g., earth rocks) behavior in response to the pressure-temperature (*P*-*T*) change is controlled by the phase equilibria, and because earth processes must leave imprints on relevant earth rocks, it is essential that we examine the LAB issue petrologically, by means of experimental petrology to constrain the phase equilibria (e.g., Green et al., 2010; Green and Falloon, 2015) and by means of petrogenesis of intra-plate ocean island basalts erupted on seafloor with age-dependent lithosphere thickness at the time of eruption (e.g., Humphreys and Niu, 2009; Niu et al., 2011). This integrated petrological study leads to the insight that the LAB is a petrological boundary controlled by the *P*-*T* change of mantle peridotite with the presence of trace amount of water.

3. The petrology of intra-plate ocean island basalts

Intra-plate ocean island basalts (OIB) are solidified melts ultimately derived from the asthenosphere and are thus expected to contain information on the asthenosphere and the LAB. Despite fine-scale complexity in the geochemistry of mantle melts, macroscopically mantle melting must leave compositional imprints on the melting product and residues which reflect the physical controls (e.g., Niu, 1997) (e.g., *P*, *T*, melt fraction *F*). For example, studies of seamounts and OIB, including magmas containing mantle-derived xenoliths, show that parental magmas (with $Mg^{\#} \approx 75$) form a continuum from extremely silica-undersaturated

(olivine melilitite and olivine nephelinite; olivine + larnite normative, and olivine + nepheline normative) through olivine-rich basanite and alkali picrite to tholeiitic picrite (olivine + hypersthene normative) (e.g., Green, 1971; Pilet et al., 2008). This sequence is one of increasing silica, alumina and decreasing Ca, Na, K and P. Most importantly, it is a sequence of decreasing dissolved C $(CO_3)^{=}$ and H $(OH)^{-}$ in the parental magmas and is experimentally shown to be decreasing pressure of melt segregation and increasing F (Green and Ringwood, 1967, 1970; Green, 1970, 1971).

Figure 2 shows correlated variations of heavily averaged global OIB compositions with the lithosphere thickness (L), which is equivalent to the LAB depth from the seafloor. The significance of these correlations can be effectively expressed in terms of the LAB (km) as a function of these compositional parameters as illustrated in Fig. 3a for two scenarios. This is the very evidence for the LAB to be the solidus. The asthenospheric mantle upwelling and decompression melting produce OIB melts, but the melting stops when the decompression-melting asthenosphere encounters the LAB. That is, the LAB caps the final depth (pressure) of melting (P_f; Fig. 3b), which is termed "lid-effect" (Ellam, 1992; Humphreys and Niu, 2009; Niu et al., 2011). OIB erupted on the thicker (older) lithosphere have geochemical characteristics of lower extent (or smaller melt fraction F; high Ti_{72}, P_{72}, $[La/Sm]_N$ and $[Sm/Yb]_N$) and higher pressure (low Si_{72} and Al_{72}, and high Fe_{72}, Mg_{72} and $[Sm/Yb]_N$) of melting because of shorter decompression melting intervals (lower $F \propto P_o$-P_f) with melt extracted at greater depths (deeper P_f). OIB erupted on thinner (younger) lithosphere have signatures of larger melt fraction (low Ti_{72}, P_{72}, $[La/Sm]_N$ and $[Sm/Yb]_N$) and lower pressure (high Si_{72} and Al_{72}, and low Fe_{72}, Mg_{72} and $[Sm/Yb]_N$) of melt extraction (Fig. 2, 3b; Niu et al., 2011) because of larger decompression melting intervals ($F \propto P_o$-P_f) with melts extracted at shallower depths (smaller P_f).

Note that melting beneath all ocean islands begins in the garnet peridotite facies (Fig. 3b), imparting the familiar 'garnet signature' to all OIB melts (e.g. $[Sm/Yb]_N > 1$; Fig. 2). The intensity of the garnet signature decreases with increasing *F* towards beneath thinner lithosphere because of the dilution effect of increased *F*, and with decrease and disappearance of residual garnet as decompression melting continues into spinel lherzolite to harzburgite residues, depending on the thickness of the lithosphere (or the LAB depth; Fig. 3b). The dilution effect is obvious for incompatible elements (e.g., K_{72}, Ti_{72}, P_{72}) and ratios (e.g., $[La/Sm]_N$) with decreasing lithosphere thickness. It is important to note also that possible variation of mantle potential temperature between ocean islands and island groups may affect the OIB compositional variation because of initial melting depth variation, but this effect is averaged out and over-shallowed by the "lid-effect" as seen in Figure 2. Mantle source heterogeneity can also impart source signature in the observed OIB compositions, but this effect, if any, can in fact enhance the "lid-effect" shown in Figures 2-3. This is because an enriched component (or enriched heterogeneities) with lower solidus temperature melts first and is concentrated in the lower-*F* melt produced beneath and erupted on the thickened (older) lithosphere, but is diluted in the higher-*F* melt produced beneath and erupted on the thin (younger) lithosphere (Fig. 2, 3b; Niu et al., 2011). The finding of the young (~ 6 Ma) "Petit Spots" with highly enriched alkali melts erupted on the 135 Ma Pacific plate (Hirano et al., 2006; Pilet et al., 2016) supports this concept, and is consistent with empirical parameterization (Green and Ringwood, 1967; Green, 1971; Jaques and Green, 1980; Niu and Batiza, 1991) of magma composition as a function of *P*, *T* and *F* based on experimental lherzolite melting and basalt liquidus studies.

In brief, the "lid-effect", as manifested by global OIB compositional systematics as a function of the lithosphere thickness in Figures 2-3, requires (1) that the LAB be a *solidus*, below which the diapirically upwelling asthenosphere melts by decompression, at which

melting stops, and above which melt freezes if not extracted through channels and conduits to the surface, and that (2) there must be a melt-rich layer right beneath the LAB (e.g., Niu and O'Hara, 2003, 2009; Niu, 2008; Humphreys and Niu, 2009; Niu et al., 2011, 2012). The latter has been detected seismically by a ~ 10% Vs drop (Kawakatsu et al., 2009).

4. Experimental petrology constraints

Geophysically, the LAB is defined as an isotherm (Fig. 1b), at least for t < ~ 70 Ma, but it is petrologically a solidus as shown above (Figs 2, 3). This requires that the solidus in question be an isotherm, i.e., dT/dP = 0 with $T_{LAB} \approx$ 1100°C, L = 0 to ~ 90 km for $t \leq$ ~ 70 Ma. Such an isothermal solidus is unexpected because the mantle solidus commonly used in models of lithosphere and asthenosphere is not an isotherm, but has $dT/dP > 0$ as illustrated by the anhydrous MORB pyrolite solidus (Fig 4a; Green and Falloon, 2015). Furthermore, the constant lithosphere thickness of L = ~ 90 km for $t \geq$ ~ 70 Ma would require the LAB, or the solidus, to be isobaric, i.e., dP/dT = 0 with $P_{LAB} \approx$ 3 GPa. All the above geophysical and petrological conditions for the LAB can only be met if the LAB represents the dehydration solidus of pargasite amphibole as illustrated in Figure 4a. That is, the lithosphere is bounded by the pargasite amphibole stability with the conditions of $T_{LAB} \leq$ 1100°C (~ 1050°C – 1150°C) and $P_{LAB} \leq$ 3 GPa (~ 0.5 – 3 GPa; ~ 90 km) (e.g., Green and Liebermann, 1976; Green et al., 2010; Niu et al., 2011).

On the origin of the asthenosphere, especially the seismic low-velocity zone (LVZ) atop the asthenosphere beneath ocean basins, some consider the possibility that the LVZ may be simply the rheologic change in response to pressure-temperature change (e.g., Stixrude and Lithgow-Bertelloni, 2005; Afonso et al., 2008a,b; Karato, 2012), but the global seafloor petrology (e.g., Niu and O'Hara, 2003, 2008, 2009; Niu and Hekinian, 2004; Niu, 2008; Humphreys and Niu, 2009; Niu and Humphreys, 2009; Niu et al., 2011, 2012), the process of

cratonic lithosphere thinning (Niu, 2014) and experimental studies require that the LVZ be characterized by the presence of a small melt fraction facilitated by a volatile phase dominated by H_2O (Green, 1970, 1971; Lambert and Wyllie, 1968, 1970; Green and Liebermann, 1976; Green et al., 2010; Green and Falloon, 2015). Indeed, the LAB matches the intersections of geotherms with the dehydration solidus of pargasite-lherzolite as indicated by the thick red dashed line (Fig. 4a). Figure 4a is a highly-simplified quantitative phase diagram (after Green and Falloon, 2015) that depicts the key elements of the oceanic upper mantle dynamics. In this context, it is conceptually and physically important to distinguish between the asthenosphere (and LAB) and the seismic low velocity zone (LVZ). The terms are often used interchangeably, but the asthenosphere, defined rheologically, is continuous globally as evidenced by the global correlation between surface elevation and lithosphere thickness (e.g., mountain belts vs. platforms, platforms/cratons vs. ocean basins). The LVZ is present beneath global ocean basins but only locally beneath continents such as eastern China, eastern Australia and western USA likely caused by water introduction associated with subducting/subducted slabs currently or in not distant past (Niu, 2014). Figure 4a shows that beneath ocean basins the lithosphere is precisely determined by the stability field of the H_2O-bearing pargasite (amphibole) in lherzolite, bounded by $T \leqslant 1100$°C and $P \leqslant 3$ GPa, i.e. the dehydration solidus (solid red dashed line) (Green and Liebermann, 1976; Niu and O'Hara, 2003; Green et al., 2010; Green and Falloon, 2015), and is controlled by the reaction:

Pargasite-bearing peridotite [lithosphere] $\Leftrightarrow$ peridotite + Melt [asthenosphere]

At depths greater than ~ 90 km, $P > 3$ GPa, pargasite is no longer stable in fertile lherzolite. If bulk water content is > ~ 200 ppm then the storage capacity of NAMs (nominally anhydrous minerals such as olivine, orthopyroxene, clinopyroxene and aluminous spinel within

the fertile lherzolite) is exceeded and water-rich vapor is present (Green et al., 2010; Green and Falloon, 2015). The vapor-saturated solidus of garnet lherzolite + H_2O is approximately 1000°C at 3 GPa and increases at higher pressure. The striking feature is the near-isothermal dehydration solidus (dT/dP ≈ 0) at $T \approx 1100$°C and $P \leqslant 3$ GPa ($\leqslant$ 90 km). Intersection of this solidus with cooling geotherms controls the LAB = 11 $t^{1/2}$ km (Fig. 3b) for seafloor of $t \leqslant 70$ Ma. Thus, ~ 70 Myrs is the time required for oceanic lithosphere to reach its 'mature' thickness of ~ 90 km as the result of conductive cooling. With $t > 70$ Ma, conductive cooling continues but the base of the lithosphere remains at ~ 90 km until the temperature at ~ 90 km drops below ~1000°C (Fig. 4a; Green and Liebermann, 1976; Niu and O'Hara, 2003; Green et al., 2010; Green and Falloon, 2015).

Figure 4b summarizes the petrological control on the LAB beneath ocean basins. The oceanic LAB is a straightforward consequence of petrological phase equilibria for lherzolite (pyrolite) with 0.02 to 0.4 wt % H_2O. This conclusion is supported by the global OIB compositional systematics (Figs. 2,3; the 'lid-effect'), by experimental petrology (Fig. 4a) and by observations from seismology, rheology, heat-flow, and electrical conductivity in the oceanic lithosphere and asthenosphere as discussed above.

5. Summary

(1) The results of many years' studies in both experimental petrology and petrogenesis of oceanic basalts have now emerged about the nature of the LAB, which is a petrological phase boundary marking the intersection of the geotherm with the dehydration solidus of amphibole (pargasite)-bearing lherzolite (Fig. 4a).

(2) The stability of the pargasite amphibole defines the oceanic lithosphere (i.e., pargasite-bearing peridotite) to be $T \leq$ ~ 1100°C, $P \leq$ ~ 3 GPa (~ 90 km). Beyond this stability field, the mantle becomes asthenosphere characterized by "dry" peridotite with an incipient melt

phase (Fig. 4a).

(3) The LAB, the amphibole dehydration solidus, is characterized by an isotherm (dT/dP = 0) of 1100°C at P ≤ ~ 3 GPa (< ~ 90 km) and an isobar (dP/dT = 0) of ~ 3 GPa (~ 90 km) at T = ~ 1050 – 1150°C (Fig. 4a,b).

(4) This understanding presents a unifying solution that not only explains why the LAB depth increases with increasing seafloor ages from beneath ocean ridges (~ 10 km) to beneath seafloors of up to ~ 70 Ma (isothermal solidus with $L \propto t^{1/2}$) on a global scale (Figs. 3,4), but also reveals the intrinsic control on the globally constant LAB depth (~ 90 km) beneath seafloors older than ~ 70 Ma (isobaric solidus at ~ 90 km) (Figs. 1,3,4).

(5) The LAB, the dehydration solidus, is an intrinsic property of lherzolite with trace amount of water. Hence, its existence *does not* require popularly invoked small-scale convection. That is, the LAB *is not* caused by the small-scale convection.

(6) However, because the mantle above the LAB is the *conductive* lithosphere and below the LAB is the *convective* asthenosphere (Figs. 3b, 4b), the viscosity-reduced asthenosphere (with incipient melt) can make small-scale convection close beneath the LAB possible under older seafloors. Such convection can indeed supply heat to balance the conductive heat loss to the seafloor, thus maintaining the constant heat flow, seafloor depth and lithosphere thickness.

(7) Therefore, (a) it is the petrological phase equilibria (Figs. 2-4) that determines the varying depth of the LAB beneath the global ocean floors, and (b) it is the LAB that makes the small-scale convection possible close beneath the LAB under ocean floors older than ~ 70 Myrs.

(8) We encourage geophysical and modeling disciplines to consider this petrological concept and conclusion presented here in their models towards an improved understanding on the nature of the LAB.

Supplementary Information (Supplements A - F**)** is available in the online version of the paper.

Acknowledgments YN thanks the international community for invited keynote presentations on the LAB concept presented here at several international conferences, including the Chinese Annual Conference on Petrology and Geodynamics in Xi'an (2011), the 34th IGC in Brisbane (2012) and Goldschmidt Conference in Sacramento (2014) as well as institutional talks at Scripps Institution of Oceanography (2015), China University of Geoscience in Beijing (2017), Chinese Geological Survey (2017), Nanjing University (2017) and Leeds University (2017). YN also acknowledges the support by National Natural Science Foundation of China (NSFC grants 41130314, 41630968), Chinese Academy of Sciences Innovation grant (Y42217101L), grants from Qingdao National Laboratory for Marine Science and Technology (2015ASKJ03) and the NSFC-Shandong Joint Fund for Marine Science Research Centers (U1606401). DHG acknowledges the support of University of Tasmania (Earth Sciences discipline) and Research School of Earth Sciences, Australian National University, in facilitating post retirement research as an honorary Professor-Emeritus. We thank two anonymous reviewers for their very detailed and constructive comments on an early version of the paper. We also thank Professor Gillian Foulger for her editorial effort.

Author Information The authors declare no conflict of interest nor competing financial interests. Correspondence and requests for materials should be addressed to Y.N. (yaoling.niu@durham.ac.uk)

References:

Afonso, J.C., Fernandez, M., Ranalli, G., Griffin, W.L., Connolly, J.A.D., 2008a. Integrated geophysical-petrological modeling of the lithosphere and sublithospheric upper mantle: Methodology and applications. Geochem. Geophys. Geosys. 9, Q05008, doi:10.1029/2007GC001834.

Afonso, J. C., Zlotnik, S., Fernandez, M., 2008b. Effects of compositional and rheological stratifications on small-scale convection under the oceans: Implications for the thickness of oceanic lithosphere and seafloor flattening. Geophys. Res. Lett. 35, L20308, doi:10.1029/2008GL035419

Ballmer M.D., van Hunen, J., Ito G., Tackley, P.J., Bianco, T.A., 2007. Non-hotspot volcano chains originating from small-scale sublithospheric convection. Geophys. Res. Lett. 34, L23310, doi:10.1029/2007GL031636.

Buck, W.R., Parmentier, E.M., 1986. Convection beneath young oceanic lithosphere: Implications for thermal structure and gravity. J. Geophys. Res. 91, 1961-1974.

Crosby, A.G., McKenzie, D., 2009. An analysis of young ocean depth, gravity and global topography. Geophys. J. Int. 178, 1198-1219.

Davies, G.F., 1988. Ocean bathymetry and mantle convection. 1. Large-scale flow and hotspots. J. Geophys. Res. 99, 10467-10480,

Davies, G.F., Richards, M.A., 1992. Mantle convection. J. Geol. 100, 151–206.

Ellam, R.M., 1992. Lithospheric thickness as a control on basalt geochemistry. Geology 20, 153-156.

Fischer, K.M., Ford, H.A., Abt, D.L., Rychert, C.A., 2010. The lithosphere-asthenosphere boundary. Ann. Rev. Earth Planet. Sci. 38, 551–575.

Forsyth, D.W., 1977. The evolution of the upper mantle beneath mid-ocean ridges. Tectonophys. 38, 89-118.

Forsyth, D., Uyeda, S., 1975. On the relative importance of the driving forces of plate motion. Geophys. J. Int. 43, 163–200.

Fowler, C.M.R., 2005. The solid Earth – an introduction to global geophysics. Cambridge University Press, New York, 2nd Edition, 685 pp.

Green, D.H., 1970. The origin of basaltic and nephelinitic magmas. Bennett Lecture, University of Leicester, Trans. Leicester Lit. Philos. Soc., 44, 28-54.

Green, D.H., 1971. Compositions of basaltic magmas as indicators of conditions of origin: application to oceanic volcanism. Philos. Trans. R. Soc. London Series A 268, 707-725.

Green, D.H., Liebermann, R.C., 1976. Phase equilibria and elastic properties of a Pyrolite model for the oceanic upper mantle. Tectonophys. 32, 61–92.

Green, D.H., Ringwood, A.E., 1967. The genesis of basaltic magmas. Contrib. Mineral. Petrol. 15, 103-190.

Green, D.H., Ringwood, A.E., 1970. Mineralogy of peridotitic compositions under upper mantle conditions, Phys. Earth Planet. Int., 3, 359-371.

Green, D.H., Falloon, T.J., 2015. Mantle-derived magmas: intraplate, hot-spots and mid-ocean ridges. Sci. Bull. 60,1873–1900.

Green, D.H., Hibberson, W.O., Kovacs, I., Rosenthal, A., 2010. Water and its influence on the lithosphere-asthenosphere boundary. Nature 467, 448-451.

Grose, C.J., Afonso, J.C., 2013. Comprehensive plate models for the thermal evolution of oceanic lithosphere. Geochem. Geophys. Geosys. 14, 3751–3778.

Hirano, N., Takahashi, E., Yamamoto, J., Abe, N., Ingle, S.P., Kaneoka, I., Hirata, T., Kimura, J.-I., Ishi, T., Ogawa, Y., Machida, S., Suyehiro, K., 2006. Volcanism in response to plate flexure. Science 313, 1426-1428.

Huang, J., Zhong, S., van Hunen, J. 2003. Controls on sublithospheric small-scale convection. J. Geophys. Res. 108, 2405.

Humphreys, E.R., Niu, Y.L., 2009. On the composition of ocean island basalts (OIB): The effects of lithospheric thickness variation and mantle metasomatism. Lithos 112, 118-136.

Jaques, A.L., Green, D.H., 1980. Anhydrous melting of peridotite at 0–15 kb pressure and the genesis of tholeiitic basalts. Contrib. Mineral. Petrol. 73, 287–310.

Karato, S., 2012. On the origin of the asthenosphere. Earth Planet. Sci. Lett. 321-322, 95-103.

Kawakatsu, H., Kumar, P., Takei, Y., Shinohara, M., Kanazawa, T., Araki, E., Suyehiro, K., 2009. Seismic evidence for sharp lithosphere-asthenosphere boundaries of oceanic plates. Science 324, 449-502.

Korenaga, T. & Korenaga, J., 2008. Subsidence of normal oceanic lithosphere, apparent thermal expansivity, and seafloor flattening. Earth Planet. Sci. Lett. 268, 41-51.

Lambert, I.B., Wyllie, P.J., 1968. Stability of hornblende and a model for the low velocity zone. Nature 219,1240-1241.

Lambert, I.B., Wyllie, P.J., 1970. Low-velocity zone of the Earth's mantle - incipient melting caused by water. Science 169, 764-766.

Lister, C.R.B., 1972. On the thermal balance of a mid-ocean ridge. Geophys. J. Int. 26, 515-535.

McKenzie, D.P., 1967. Some remarks on heat flow and gravity anomalies. J. Geophys. Res. 72, 6261–6273.

McKenzie, D., Bickle, M.J., 1988. The volume and composition of melt generated by extension of the lithosphere. J. Petrol. 29, 625–679.

McKenzie, D.P., Jackson, J., Priestley, K., 2005. Thermal structure of oceanic and continental lithosphere. Earth Planet. Sci. Lett. 233, 337-349.

Niu, Y.L., 1997. Mantle melting and melt extraction processes beneath ocean ridges: Evidence from abyssal peridotites. J. Petrol. 38, 1047–1074.

Niu, Y.L., 2008. The origin of alkaline lavas. Science 320, 883-884.

Niu, Y.L., 2014. Geological understanding of plate tectonics: Basic concepts, illustrations, examples and new perspectives. Global Tectonics and Metallogeny 10, 23-46.

Niu, Y.L., 2016. The meaning of global ocean ridge basalt major element compositions. J. Petrol. 57, 2081-2104.

Niu, Y.L., Batiza, R., 1991. An empirical method for calculating melt compositions produced beneath mid-ocean ridges: Application for axis and off-axis (seamounts) melting. J. Geophys. Res. 96, 21753-21777.

Niu, Y.L., Hékinian, R., 2004. Ridge suction drives plume-ridge interactions. In Oceanic Hotspots, edited by Hékinian, R., Stoffers, P., Cheminee, J.-L., Springer-Verlag, New York, p. 285-307.

Niu, Y.L., Humphreys, E., 2009. On the origin of OIB and LVZ – Some new perspectives. Goldschmidt Conference Abstract, A948.

Niu, Y.L., O'Hara, M.J., 2003. Origin of ocean island basalts: A new perspective from petrology, geochemistry and mineral physics considerations. J. Geophys. Res. 108, 2209, doi:10.1029/2002JB002048.

Niu, Y.L., O'Hara, M.J., 2008. Global correlations of ocean ridge basalt chemistry with axial depth: A new perspective. J. Petrol. 49, 633-664.

Niu, Y.L., O'Hara, M.J., 2009. MORB mantle hosts the missing Eu (Sr, Nb, Ta and Ti) in the continental crust: New perspectives on crustal growth, crust-mantle differentiation and chemical structure of oceanic upper mantle. Lithos 112,1-17.

Niu, Y.L., Wilson, M., Humphreys, E.R., O'Hara, M.J., 2011. The Origin of Intra-plate Ocean Island Basalts (OIB): The lid effect and its geodynamic implications. J. Petrol. 52, 1443–1468.

Niu, Y.L., Wilson, M., Humphreys, E.R., O'Hara, M.J., 2012. A trace element perspective on the source of ocean island basalts (OIB) and fate of subducted ocean crust (SOC) and mantle lithosphere (SML). Episodes 35, 310-327.

Parsons, B., McKenzie, D., 1978. Mantle convection and the thermal structure of the plates. J. Geophys. Res. 83, 4485–4496.

Parsons, B., Sclater, J.G., 1977. An analysis of the variation of ocean floor bathymetry and heat flow with age. J. Geophys. Res. 82, 803-827.

Phipps Morgan, J., Smith, W.H.F., 1992. Flattening of the sea-floor depth-age curve as a response to asthenospheric flow. Nature 359, 524-527.

Pilet, S., Abe, N., Rochat, L., Kaczmarek, M.-A., Hirano, N., Machida, S., Buchs, D.M., Baumgartner, P.O., Müntener, O., 2016. Pre-subduction metasomatic enrichment of the oceanic lithosphere induced by plate flexure. Nature Geosci. 9, 898-903.

Pilet, S., Baker, M.B., Stolper, E.M., 2008. Metasomatized lithosphere and the origin of alkaline lavas. Science 320, 916-919.

Sclater, J.G., Francheteau, J., 1970. The implications of terrestrial heat-flow observations on current tectonic and geochemical models of the crust and upper mantle of the earth. Geophys. J. Int. 20, 493–509.

Sclater, J.G., Jaupart, C., Galson, D., 1980. The heat flow through oceanic and continental crust and the heat loss of the earth. J. Geophys. Res. 18, 269-311.

Sleep, N.H., 1969. Sensitivity of heat flow and gravity to the mechanism of sea-floor spreading. J. Geophys. Res. 74, 542-549.

Sleep, N.H., 1987. Lithosphere heating by mantle plumes. J. Geophys. Res. 91, 1-11,

Sleep, N.H., 2011. Small-scale convection beneath oceans and continents. Chinese Sci. Bull. 56, 1292–1317.

Stein, C.A., Stein, S., 1992. A model for the global variation in oceanic depth and heat flow with lithospheric age. Nature 359, 123–129.

Stein, S., Stein, C.A., 1996. Thermo-mechanical evolution of oceanic lithosphere: implications for the subduction processes and deep earthquakes. Am. Geophys. Uni. Monogr. 96, 1-17.

Stixrude, L, Lithgow-Bertelloni, C., 2005. Mineralogy and elasticity of the oceanic upper mantle: Origin of the low-velocity zone. J. Geophys. Res. 110, B03204, doi:10.1029/2004JB002965

Wood, B.J., Yuen, D.A., 1983. The role of lithosphere phase transitions on seafloor flattening at old ages. Earth Planet. Sci. Lett. 66, 303-314.

Figure captions:

Figure 1. ***a***, Global seafloor mean depth (D) variation with age (t) (data from Crosby and McKenzie (2009)), which is effectively described by the half-space cooling model (HSM, $D \propto t^{1/2}$) for seafloor with $t \leqslant \sim 70$ Ma. Conductive cooling continues but seafloor depth

flattens when t > 70 Ma. ***b***, With the base of the lithosphere (i.e., the LAB, the depth below seafloor) as an isotherm (e.g., 1100°C from Fowler (2005)), the HSM well describes the lithosphere thickness $L \propto t^{1/2}$ (or $L = 11t^{1/2}$) for $t \leqslant$ 70 Ma, but fails to explain the approximately constant thickness of ~ 90 km (Stein and Stein, 1996) for t > 70 Ma. Plate models (PM) (e.g., Forsyth, 1977; Parsons and McKenzie, 1978; Stein and Stein, 1996; McKenzie et al., 2005; Sleep, 2011) have thus been advocated to account for lithosphere thickness variation of all ages. Many versions of PM models exist, but we plot a few for comparison with assumed basal isotherms of 1100°C and 1200°C respectively (e.g., McKenzie et al., 2005; Grose and Afonso, 2013). The 1100°C (red) and 1200°C (blue) isotherm models (Kawakatsu et al., 2009) represent actual depths of the LAB obtained seismically characterized by ~ 10% sudden Vs drop, consistent with the LAB being a natural solidus and the presence of a melt-rich layer atop the asthenosphere of all seafloor ages in order to fully explain the oceanic petrogenesis (Niu and O'Hara, 2003, 2008, 2009; Niu, 2008; Niu et al., 2011). We note the large uncertainties in earlier model estimates. For example, Parson and Sclater (1977) suggested plate thickness of L = 125±10 km with basal T = 1350±275°C, whereas Stein and Stein (1996) suggested L = 95±15 km with basal T = 1450±250°C because of lacking solid constraints. The petrological results presented in this paper place constraints on $L \approx$ 90 km with basal T ≈ 1100°C. We also note the earlier interpretation that the seafloor flattening could be caused by mantle plume heating and oceanic plateaus (Sleep, 1987; Davies, 1988; Korenaga and Korenaga, 2008), but this is globally unsupported.

Figure 2. Variation of average compositions of global ocean island basalt (OIB) geochemistry as a function of lithosphere thickness (the depth of the LAB below seafloor) at the time of OIB eruption (modified from Humphreys and Niu (2009); Niu et al. (2011)). The heavy averaging was done for 10-kilometer lithosphere thickness intervals using 12996 samples from 115 ocean

islands with known seafloor ages (used to calculate $L = 11t^{1/2}$) at the time of OIB eruption from the Pacific, Atlantic and Indian oceans (see Supplements A-C, E for data details). The subscript 72 refers to corresponding oxides (SiO_2, TiO_2, Al_2O_3, FeO, MgO, CaO, P_2O_5) corrected for fractionation effect to a constant $Mg^{\#} = 0.72$ (Humphreys and Niu, 2009; Niu et al., 2011; Supplements B,D). The subscript N refers to rare earth element ratios La/Sm and Sm/Yb normalized to C1 chondrite following the tradition (Supplement C). The correlation coefficients are statistically significant at confidence levels as indicated. The blue symbol at L = 90 km indicates the lithosphere on which sampled islands older than > 70 Ma is all assumed to have thickness of ~ 90 km, which is expected (see Stein and Stein, 1996), with the OIB compositional variability (2σ variation) no greater than that for younger and thinner lithosphere.

Figure 3. ***a***, two scenarios of the LAB (km, depth below seafloor) expressed in terms of OIB compositional data in Fig. 2 using multi-variate regressions (see Supplement E). ***b***, cartoon illustrating the meaning of the data in Figs 2 and 3a. In OIB genesis, episodic magmatism, sea-mounts and island chains, and heterogeneity in magma type, trace element and isotopic signatures, suggest small scale upwelling or diapirs. This contrasts with near-continuous magmatism and larger melt fraction in MORB petrogenesis. We designate P_o (~ "dry solidus") as the pressure (depth) within the asthenosphere from which diapiric upwelling/melting begins. Melt fraction (F) increases within the upwelling/decompression melting diapir until the diapir encounters the LAB (designated P_f), where melting stops with effective melt extraction through lithospheric channels/conduits. The melt fraction (F) is proportional to decompression intervals (P_o-P_f). This is the "lid effect" (Niu et al., 2011). The pressure recorded in the OIB geochemistry is P_f, the final depth of melt-solid equilibration. This is super-imposed on a 'mantle source' signature expressing the pre-upwelling history and heterogeneity within the asthenosphere. OIB erupted on older and thickened lithosphere have signatures of lower F

(higher Ti_{72}, P_{72}, $[La/Sm]_N$ and $[Sm/Yb]_N$) and higher P (low Si_{72} and Al_{72}, high Mg_{72} and Fe_{72}) of melt extraction, whereas OIB erupted on younger and thin lithosphere have the reverse. The green layer (Fig. 3b) beneath the LAB indicates the presence of a melt-rich layer (supplied by the rising incipient melt denoted by the green arrowed wavy lines), which is required to explain the compositional systematics of oceanic basalts (Niu and O'Hara, 2003, 2009; Niu and Hekinian, 2004; Niu, 2008; Pilet et al., 2016) and is observed seismically (Kawakatsu et al., 2009). Note the position of the garnet/spinel lherzolite phase boundary is such that asthenospheric melting all begins (P_o) in the garnet lherzolite stability field, and melt segregation/extraction from the upwelling/diapiric asthenosphere may occur throughout until the melting cessation capped by the lid (P_f) in the stability fields of garnet, spinel and plagioclase lherzolite, depending on the thickness (and age) of the lithosphere. The blue-arrowed dash lines indicate plate-separation induced asthenosphere flow toward ridges (Niu and Hékinian, 2004) with small arrows indicating sub-ridge extraction of dominantly depleted (red) and minor enriched (green) melts parental to MORB.

Figure 4. ***a***, A modified model (after Green and Falloon, 2005) to show the thermal and dynamic structure of the Earth's uppermost mantle based on experimental determination of phase assemblages, solidus and melt compositions of ideal mantle lherzolite (i.e., MORB pyrolite) with the presence of minor volatiles (H_2O, CO_2 and other H-C-O species) dominated by H_2O. All the elements are self-explanatory as labeled or indicated. We emphasize that the oceanic lithosphere is defined by the pargasite (amphibole) stability field with $T \leqslant 1100$°C and $P \leqslant 3$ GPa, beyond which pargasite becomes unstable and the pargasite-bearing lithosphere becomes asthenosphere with the presence of a minor melt phase. The key is the pargasite dehydration solidus indicated with thick red dashed line: (1) $dT/dP \approx 0$ at $T \approx 1100$°C and (2) $dP/dT \approx 0$ at $P \approx 3$ GPa (~ 90 km). The scenario (1) explains LAB $\approx 11t^{1/2}$ (km) for

seafloor of t < 70 Ma, and the scenario (2) explains why the LAB ≈ 90 km for seafloor of t > 70 Ma. Note that the recently seismically detected LAB beneath the mature lithosphere is ~ 80 - 85 km in depth (Kawakatsu et al., 2009). This is not inconsistent with the ~ 90 km, but within the uncertainties of seismic models and experimental petrology. Importantly, the presence of sub-solidus carbonate (i.e. relatively oxidised and without graphite or methane) may cause the minute carbonatite melt within pargasite-bearing lherzolite in the lower lithosphere. This has consequences for electrical conductivity, and possibly rheology and seismic properties near the LAB. The pressure effect ~ of 5.5 km seawater column is equivalent to 1.65 km of rock column and can be neglected within the overall uncertainties. ***4b***, Semi-quantitative illustration on the nature of the LAB controlled by petrological phase equilibria as depicted in Figs. 2-3, 4***a***.

Figure 1 (Niu & Green, 2017)

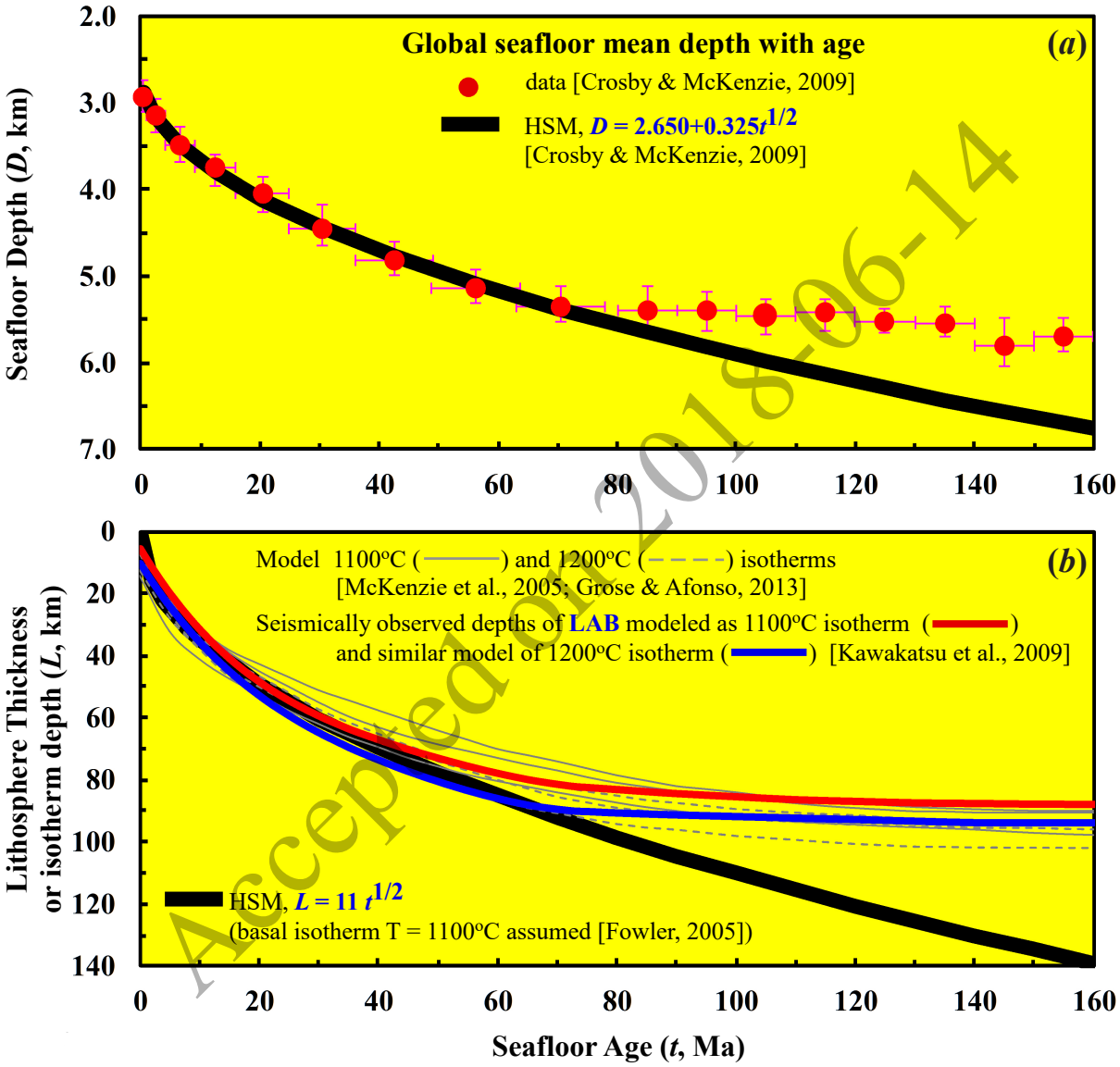

Figure 2 (Niu & Green, 2017)

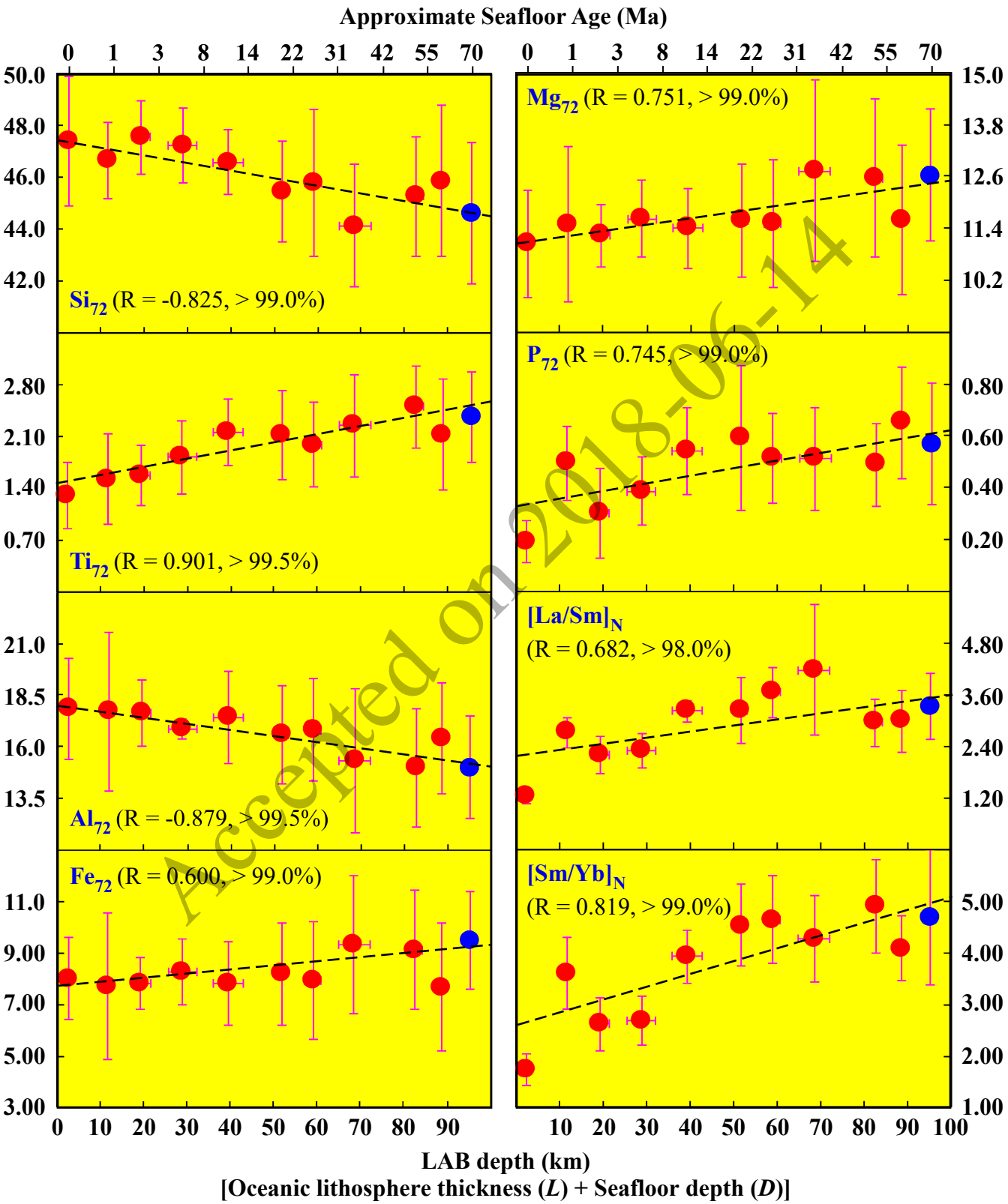

Figure 3 (Niu & Green, 2017)

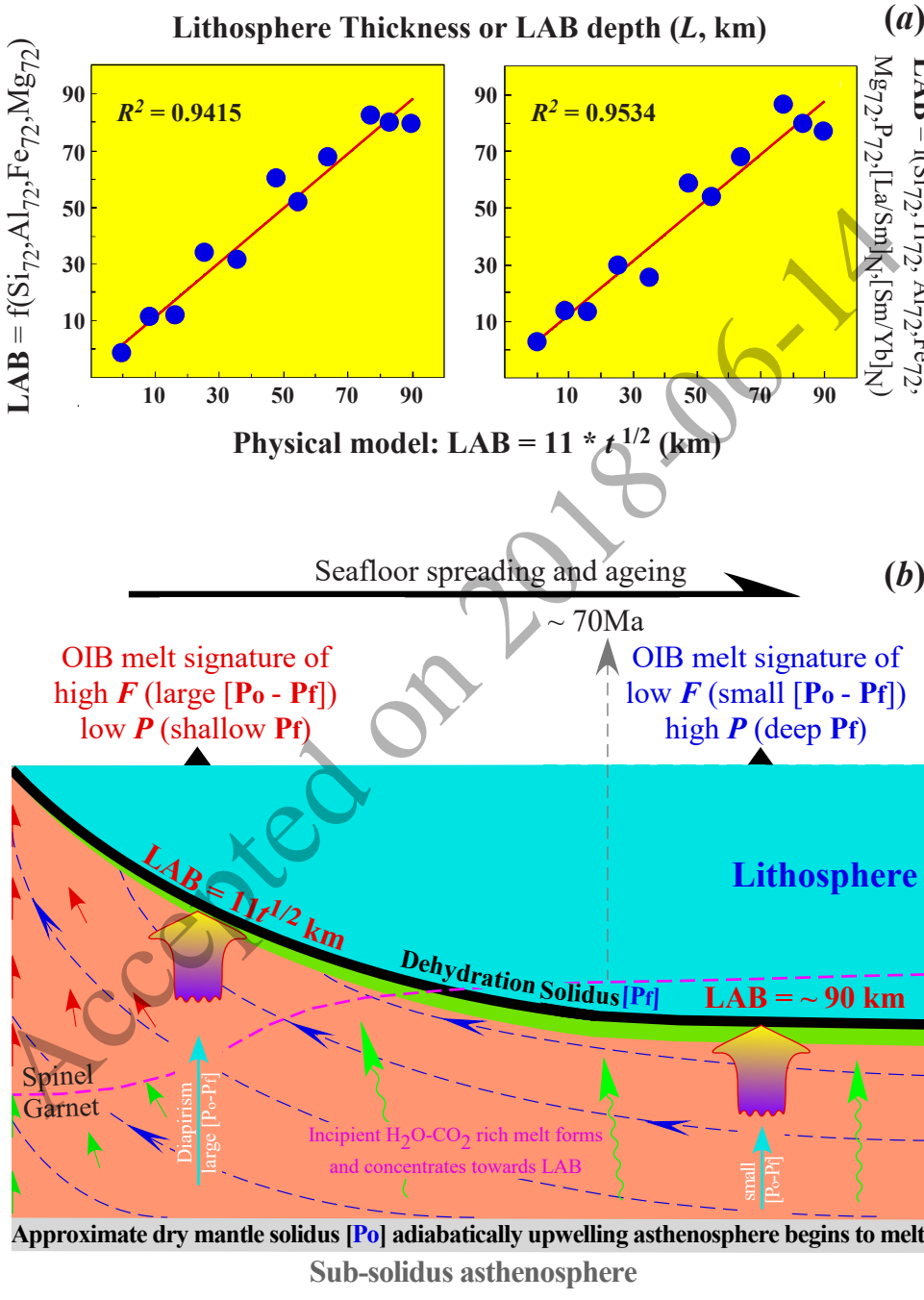

Figure 4 (Niu & Green, 2017)